

# **DSP IMPLEMENTATION OF FUZZY LOGIC-BASED LOAD VOLTAGE STABILIZATION CONTROL**

**E. E. EL-Kholy, A. EL-Sabbe, S. S. Shokralla, and  
Nancy A. EL-Hefnawy**

*Electrical Engineering Departement, Faculty of Engineering,  
Menoufiya University Shebin El-Kom, Egypt.*

## **ABSTRACT:**

This paper presents a simplified control model for stabilizing a load voltage using a switched reactor in parallel with a fixed capacitor of static VAR compensator. Two IGBT's are used to control the reactance of the switched reactor. A uniform pulse width modulation (UPWM) is used for controlling the two switches. The load is static and/ or dynamic, and the supply impedance is taken into account. The system parameters are selected according to the load. This compensator has a simple control circuit and structure. The load voltage and power factor are improved. Also, the supply input waveforms are found to be nearly sinusoidal. A complete modeling and numerical simulation for the proposed systems are presented.

A high speed Digital Signal Processor is used for implementing proportional-integral (PI) and fuzzy load voltage controllers. The system behavior is obtained under both transient and steady-state conditions. The steady-state waveforms are analyzed into their harmonic contents. Experimental results indicate the superiority of fuzzy logic control over the conventional proportional-integral control methods. Simulation results are reported and proved to be in good agreement with the relevant experimental results.

**KEYWORD:** Fuzzy logic control, VAR compensation, Load voltage stabilization.

---

Manuscript received from Dr. A.El - Sabbe

Accepted on : 15 / 6 / 2002

Engineering Research Journal Vol 25, No 3, 2002 Minufiya University, Faculty Of  
Engineering , Shebien El-Kom , Egypt , ISSN 1110-1180

## 1. INTRODUCTION:

In recent years there has been a substantial increase in the demand for controllable reactive power sources which can regulate and stabilize transmission and distribution lines and can compensate for large intermittent lagging loads. The power compensation requirements involve precise and continuous reactive power control with fast response, avoidance of harmonic line current generation[1]. Most electrical networks are subjected to loads such as furnaces and rolling mills which impose rapid variation of reactive power, which in turn cause voltage fluctuations and lamp flicker[2].

A number of papers discuss various static VAR compensator topologies based on force commutated voltage source inverter. The authors have proposed a scheme that uses a filter reactor on the line side and self controlled dc bus[2]. The modulation index is controlled directly by the VAR calculator. The scheme allows the use of optimized PWM patterns for harmonic rejection and is suitable for slowly varying VAR demand applications. In reference[3], the modulation index is fixed and the capacitor voltage is controlled so that the inverter output voltage matches in magnitude the line voltage. Capacitor voltage control is achieved through phase shifting of the inverter voltage with respect to the line voltage. In spite of its simplicity, the load angle control scheme does not allow very fast response to be achieved particularly at high power ratings[3]. Thyristors controlled reactors are a source of harmonics distortion in power systems.

In reference[4], two filter arms are considered; one is tuned for third harmonic frequency and other is for the fifth one. These filters are used to eliminate the third and fifth current harmonics as well as reducing the terminal voltage distortion. Synchronous compensators, mechanically switched capacitors and inductor and saturated reactors have been applied for many years to control the system voltage. Also, thyristor controlled reactor (TCR) devices together with fixed capacitors (FC) or thyristor – switched capacitors (TSC) have been used. The rating of inductors and capacitor used in the TCR/FC or TCR/TSC scheme, in most cases, exceeds the reactive power supplied or absorbed by the scheme. This leads to considerable expenses and large requirement for land on which to locate the compensator [5]. Steady-state characteristics are reported for open loop systems for switch reactor based static VAR compensators [6]. In reference [7], a static reactive power compensator is designed to be capable of supply both balanced and unbalanced reactive power demands. In reference [8], error-driven, error-scaled, self-adjusting SVC-control strategy is driven by the presence of a nonlinear dynamic loads. This control ensures adequate compensation level and damping effectiveness at all times based on the magnitude of the excursion error deviation-vector in the error hyperplane.

In this paper an efficient switched reactor in parallel with a capacitor for static VAR compensator is presented. To overcome the low-order harmonics and slow response associated with the conventional thyristor controlled reactor

compensators, the amplitude pulse width modulation is used for controlling the reactance of the switched reactor. The total harmonic distortion factor for load voltage and supply current are obtained for the proposed system. The proposed system is implemented using a high speed digital signal processor (DSP) for PI and/or fuzzy logic load voltage controllers. The system behavior under steady-state and transient condition is obtained and proved the superiority of the fuzzy logic controller over the conventional PI controller method. There are agreement between the simulation and experimental results.

## 2. DESCRIPTION OF THE SYSTEM

The system under consideration is illustrated in Fig. 1. The system consists of two switched reactors, a fixed capacitance and load; all of them are in parallel. However, two self-commutated bi-direction IGBT switches are used to control the reactance of the switched reactor. The simulation and experimental results are verified using an inductive load and /or dynamic load. The source reactance is taken 15 % to 20 % of the load impedance and the source resistance is taken 10 % of the source reactance [4]. The values of the controlled reactance and capacitance of the compensator are selected according to the following relationship [4,9]:

$$\omega c = \frac{1}{\omega L_0} = \frac{1}{z_l} \sin\phi_l \quad (1)$$

The parameter values of the designed system are given in the Appendix. The differential equations which describe the mode of operation for this system are given in reference[10]. The gate pulses are achieved by comparing the controller output with the triangular carrier signal using the DSP. The operation principle of the proposed system can be illustrated in Fig. 1. The two switches  $Q_1$  and  $Q_2$  represent two self-commutated bi-directional switches. Switch  $Q_2$  is used to free-wheel the controlled inductor current ( $i_{L0}$ ) when  $Q_1$  is off. Through high frequency switching, the fundamental component of the inductor current ( $i_{L0}$ ) can be controlled by controlling the output, to stabilize the load voltage at constant value.

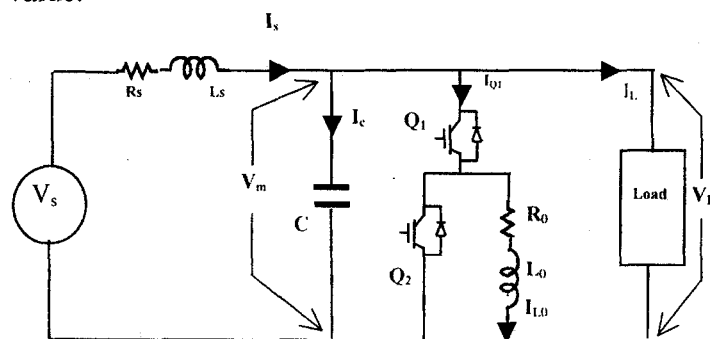


Fig. 1. Schematic diagram of proposed system.

### 3. FUZZY CONTROLLER FOR LOAD VOLTAGE STABILIZATION

The inputs of the fuzzy controller are the error  $e(k)$  and the change of error  $ce(k)$ , which are defined as:

$$e(k) = V_{ref} - V_m(k) \quad (2)$$

$$ce(k) = e(k) - e(k-1) \quad (3)$$

where  $V_m(k)$  is the present load voltage  $V_{ref}$  is the reference voltage, and the subscript  $k$  denotes values taken at the beginning of the  $k^{th}$  switching cycle. The output of the fuzzy controller is the control voltage and is defined as:

$$V_c(k) = V_c(k-1) + \xi \Delta V_c(k) \quad (4)$$

where  $\Delta V_c(k)$  is the inferred change of control voltage by the fuzzy controller at the  $k^{th}$  sampling time, and  $\xi$  is the gain factor of the fuzzy controller. Adjusting  $\xi$  can change the effective gain of the controller.

The values of  $e(k)$ ,  $ce(k)$  and  $\Delta V_c(k)$  are normalized. The triangular shape of the membership functions of this arrangement presumes that for any particular input there is only one dominant fuzzy subset. Also for any combination of  $e$  and  $ce$ , a maximum of four rules are adopted.

The derivation of the fuzzy control rules is heuristic in nature and based on the following criteria:

- 1- When the load voltage of the common coupling bus-bar is far from the set point, the change of control signal must be large so as to bring the output to the set point quickly.
- 2- When the load voltage of the common coupling bus-bar is approaching the set point, a small change of control signal is necessary.
- 3- When the load voltage of the common coupling bus-bar is near the set point and is approaching it rapidly, the control signal must be kept constant so as to reduce overshoot.
- 4- When the set point is reached and the output input still changing, the control voltage must be changed a little bit to prevent the load voltage from moving away.
- 5- When the set point is reached and the load voltage is steady, the control voltage remains unchanged.
- 6- When the load voltage is above the set-point, the sign of the change of control voltage must be negative.
- 7- When the load voltage is below the set-point, the sign of the change of control voltage must be positive.

The inference result of each rule consists of two parts, the compatibility (weighting factor)  $w_i$  of the individual rule, and the degree of change of control signal  $C_i$  according to the rule. The weighting factor  $w_i$  is obtained by applying the minimum operation on the  $\mu(e_0)$  and  $\mu(ce_0)$ , where  $e_0$  and  $ce_0$  are the

singleton inputs of  $e$  and  $ce$ .  $C_i$  is obtained from the rules, which show the mapping from the product space of  $e$  and  $ce$  to  $C_i$ . The inferred output of each rule can therefore be written as:

$$\Delta V_{ci} = \min \{ \mu_c(e_0), \mu_{ce}(ce_0) \} C_i = w_i C_i \quad (5)$$

Where  $\Delta V_{C_i}$  denotes the change of control signal inferred by the  $i^{\text{th}}$  rule. After collecting all the results, a crisp value of the change of control voltage can be obtained. Here the method of the center of gravity is preferred. The resultant change of control signal can be found as:

$$\Delta V_c(k) = \frac{\sum_{i=1}^N \Delta V_{ci}}{\sum_{i=1}^N w_i} = \frac{\sum_{i=1}^N w_i C_i}{\sum_{i=1}^N w_i} \quad (6)$$

Where  $N$  is the maximum number of effective rules.

#### 4. EXPERIMENTAL SET-UP

The experimental set-up is shown in Fig. 2, the load is static and/or dynamic. A universal motor under test is coupled to a self-excited dc generator, which acts as a load. An incremental encoder is coupled to the motor shaft to measure the motor speed. The load, supply and compensator current are sensed using hall-effect transducers, which have good linear response over wide range. Also, the load and supply voltages are sensed using voltage transducer, which has good linear response over wide range. This system is fully controlled by using dSPACE DS1102 [11] controller board which is installed on a PC computer.

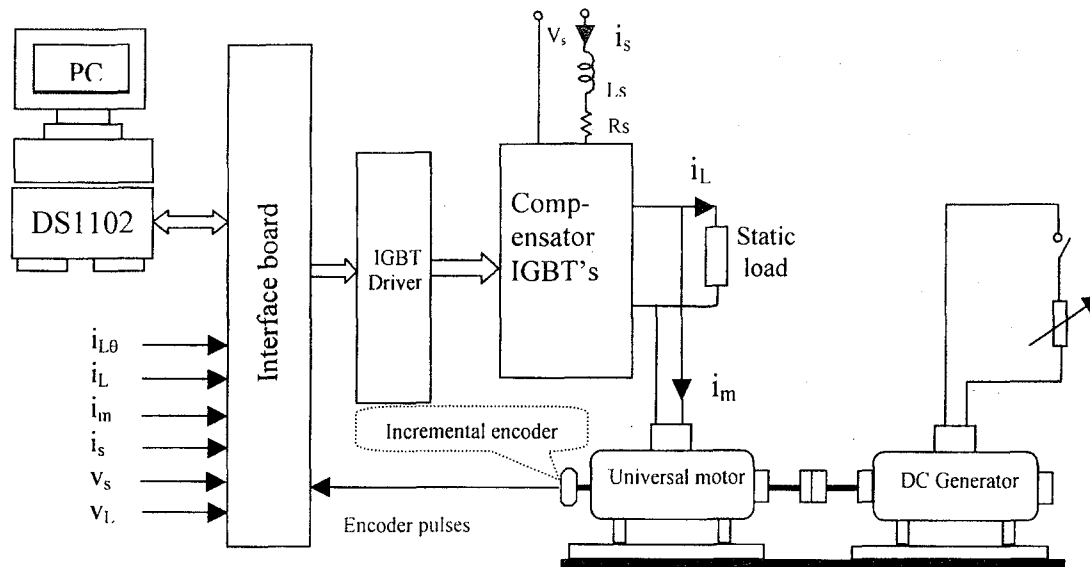


Fig. 2. Experimental set-up for DSP-based control

The controller board DS1102 is specifically designed for the development of high-speed multi-variable digital controllers and real time implementation. The DS1102 board is based on Texas instrument TMS320C31 floating-point digital signal processor (DSP) which represents the processing unit. The DSP has been supplemented by a set of on-board peripherals used in digital control systems, such as analog to digital converters (A/D), digital to analog converters (D/A) and incremental encoder interface. The board includes a DSP micro controlled based digital I/O subsystem as shown in Fig. 2. This micro controller is based on TMS320P14 processor and it can be used as a slave processor on the board. The DS1102 board can be installed on a PC with capability of uninterrupted communication with the latter through the dual-port memory, that can be used by the DSP monitor on the host PC. The feedback signals to the controller board are the measured load voltage, supply voltage, the motor shaft speed, load current, compensator current and supply current. The actual currents are measured using Hall-effect devices. The currents are then buffered and fed to the A/D converters on the board. The motor speed is measured by an optical incremental encoder installed at the motor shaft. The encoder generates 2048 pulses per revolution. A 24-bit up-down counter is used to count the encoder pulses and is read by calling function in the software. The output of the controller board in the form of digital pulses is sent directly to the base drive circuit of the IGBT's.

## 5. SIMULATION AND EXPERIMENTAL RESULTS

The proposed system is designed and implemented using DSP to verify the load voltage control requirements with PI controller and/or fuzzy logic controller. The behavior of this system under steady-state and transient conditions are obtained for static inductive load. The system has been tested using dynamic load, which is the universal motor. These results show the accuracy of the developed simulation when compared with the experimental results.

### 5.1. Open –loop UPWM with static load

Figure 3 shows the experimental waveforms of the supply voltage ( $v_s$ ) and current ( $i_s$ ) with duty ratio equal to 0.7. It is observed that the power factor at common coupling bus-bar near unity power factor. Also, it is clear that the supply voltage and current waveforms are sinusoidal.

Figure 4 shows the simulation and experimental waveforms of the load voltage ( $v_L$ ) and current ( $i_L$ ). It is noticed that the waveforms are sinusoidal. Figure 5 shows the experimental load voltage ( $v_L$ ), compensator inductor current ( $I_{L0}$ ) and switch  $Q_1$  current ( $i_{Q1}$ ). It is observed that the inductor current lags the common coupling load voltage by  $90^\circ$ .

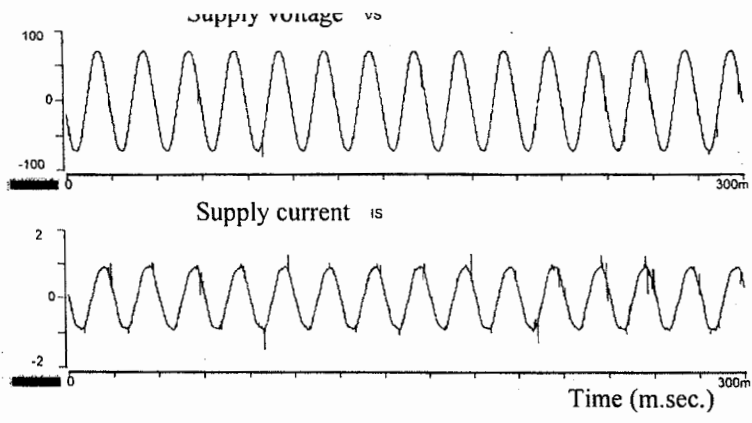
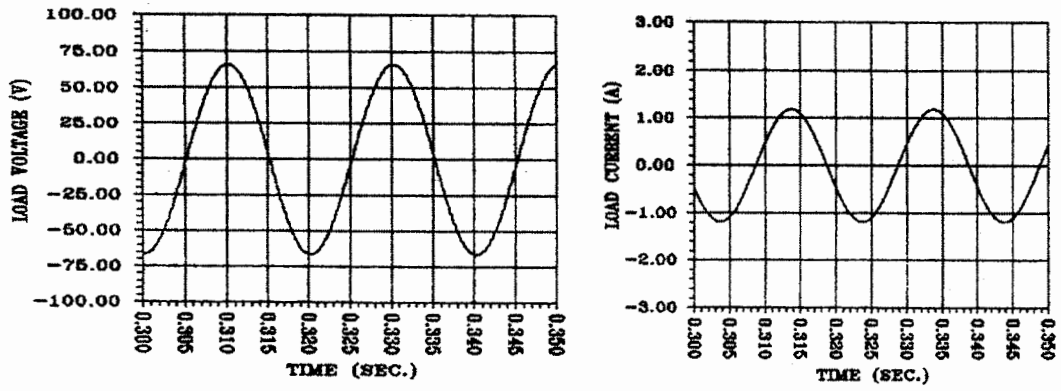
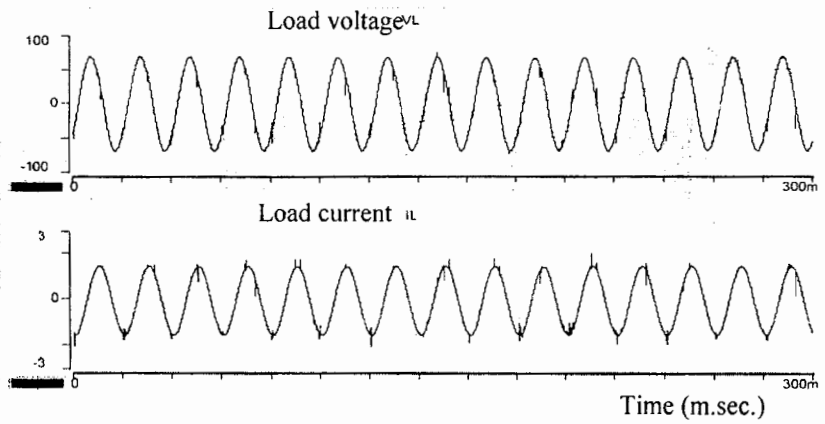


Fig. 3. Experimental waveforms for supply voltage and current.



(a) Simulation



(b) Experimental

Fig. 4. Simulation and experimental results for load voltage and current.

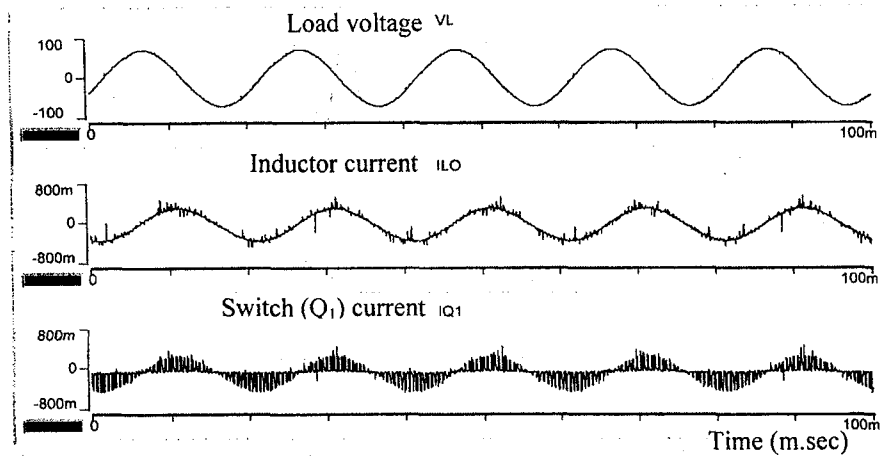


Fig. 5. Experimental waveforms for load voltage, inductor and switch current.

## 5.2. Closed loop PI controller for static load

### 5.2.1. Reference voltage step change

Figures 6 and 7 show the variation of the load rectified output voltage sensor and the load current due to positive and negative step change in reference voltage for  $K_p=5$  and  $K_i=0.1$

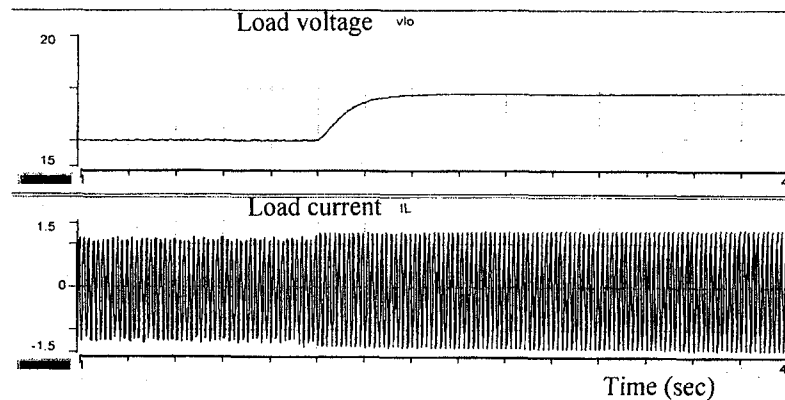


Fig. 6. Variation of the load voltage and current due to a positive step change in reference voltage

### 5.2.2. Load change

Figure 8 shows the variation of the rectified load output voltage sensor, the control voltage and the load current due to positive and negative load change ( $K_p=5$ ,  $K_i=0.1$  sec).

### 5.2.3. Open and closed loop Run-up for the Universal motor:

Figures 9 and 10 show open and closed loop run-up behavior of the universal motor as a dynamic load with the PI controller. It is observed that the run-up



time for closed loop system is decreased and the common coupling bus bar voltage remains constant.

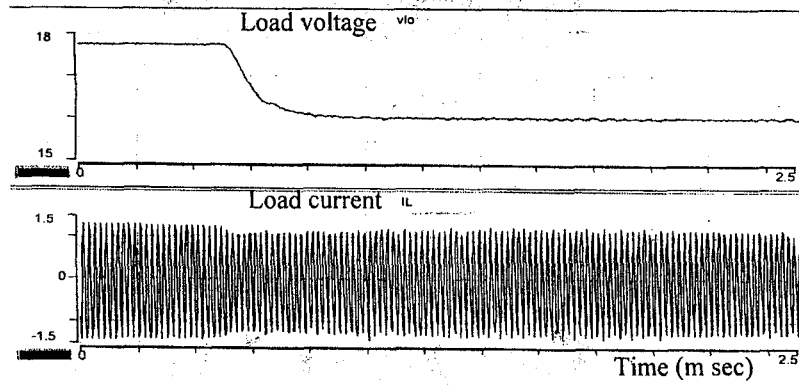


Fig. 7. Variation of the load voltage and current due to a negative step change in reference voltage

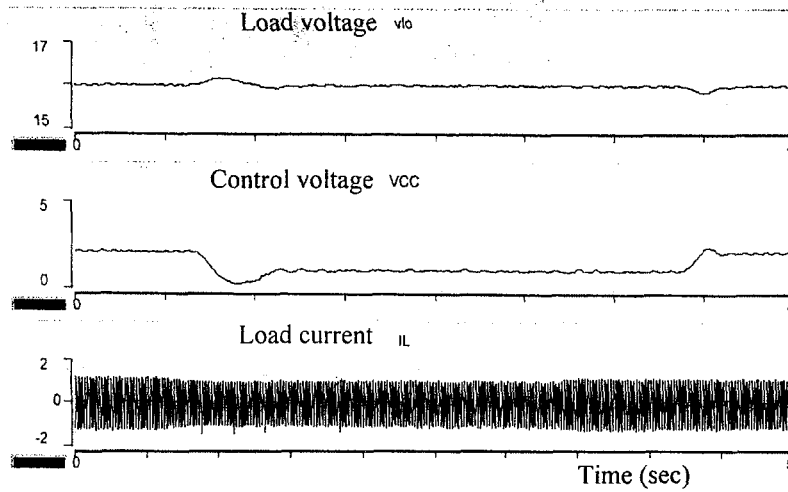


Fig. 8. Variation of load voltage and control voltage due to positive and negative load change

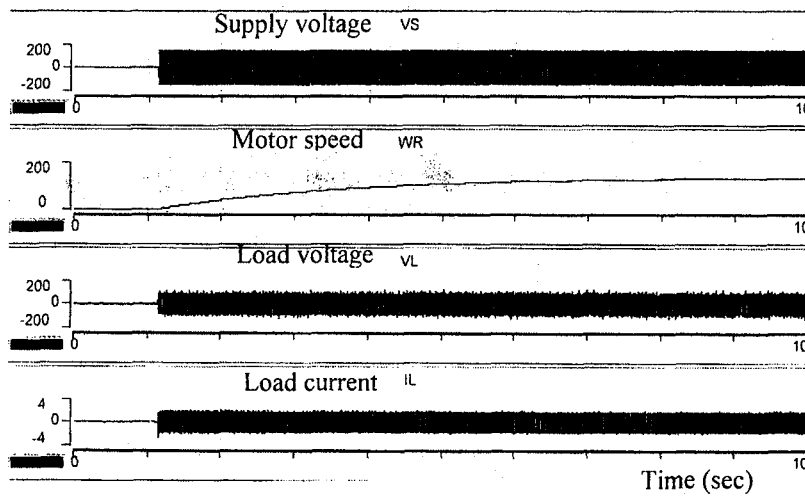


Fig. 9. Open loop run-up behavior for half load

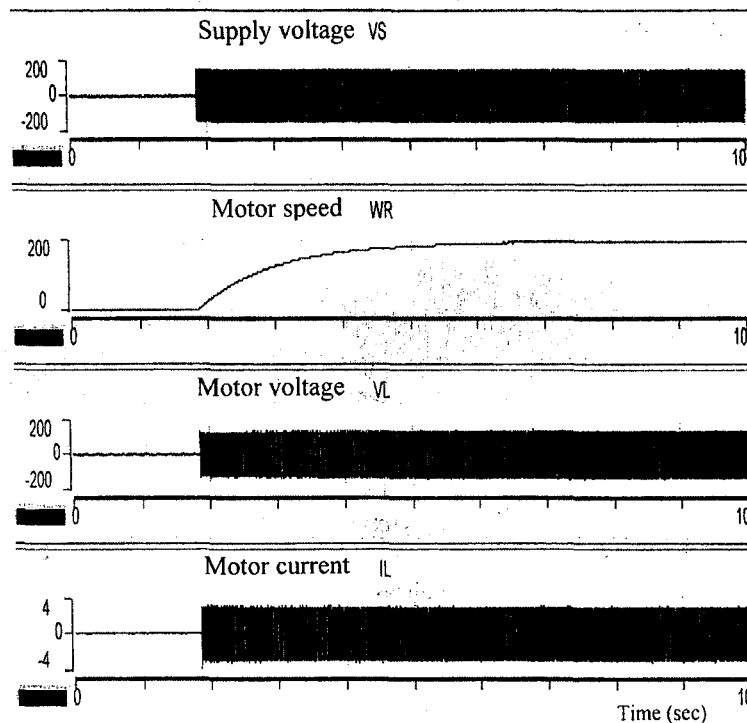


Fig. 10. Closed loop run-up behavior for half load and  $V_{ref}=140$  volt.

### 5.3. Closed loop fuzzy logic controller

The effectiveness of the proposed fuzzy logic controller on the transient and dynamic characteristics of the load voltage stabilization is investigated.

#### 5.3.1. Reference voltage step change for static load

Figures 11 and 12 show the responses of the common coupling bus-bar rectified load output voltage sensor, and the control voltage due to positive and negative step change in the reference voltage for closed-loop fuzzy control system. It is noticed that the response is faster than the PI controller.

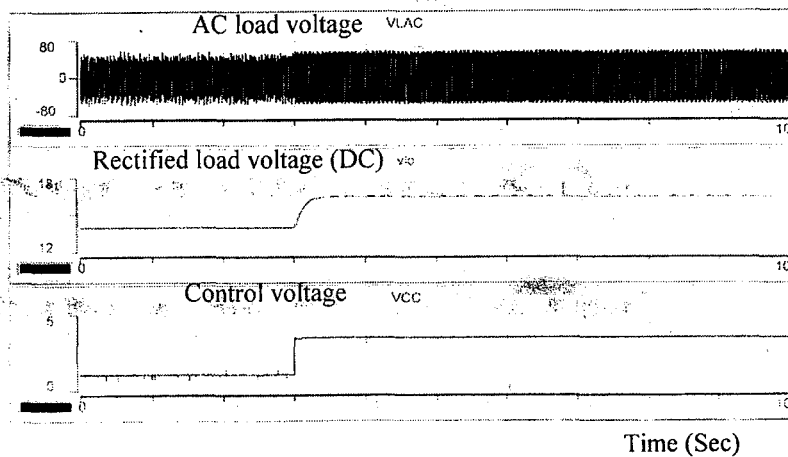


Fig. 11. Responses due to positive step change in reference voltage

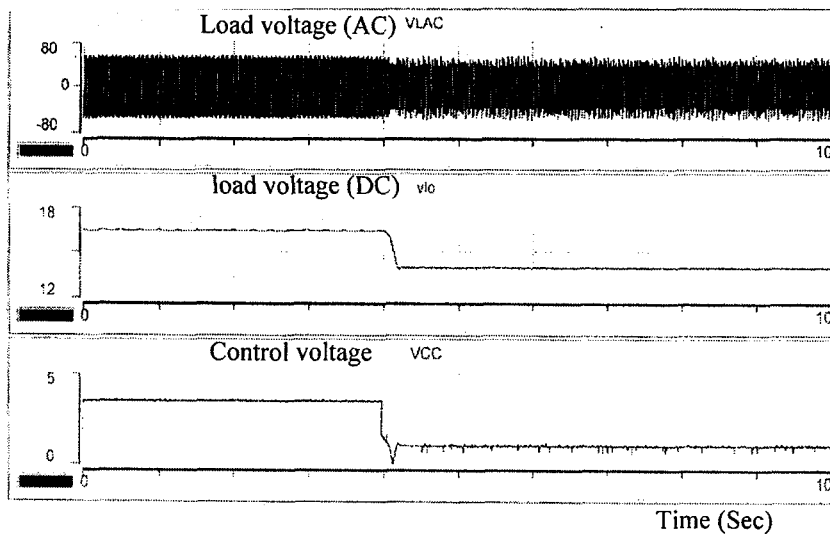


Fig. 12. Responses due to negative step change in reference voltage

### 5.3.2. Static load change

Figures 13 shows the response of the common coupling bus-bar rectified load voltage sensor, load current and control voltage due to positive and negative load change for closed-loop voltage stabilization using fuzzy control system. It is clear that the response with fuzzy control is faster than with the PI controller and the load voltage is constant.

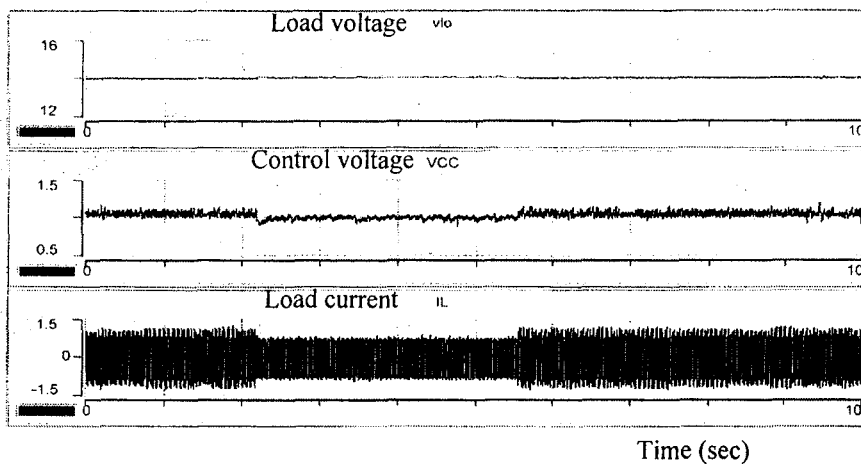


Fig. 13. Variations of load current, load voltage and control voltage due to positive and negative load change for closed loop fuzzy control.

### 5.3.3. Motor run-up using fuzzy control

Figure 14 shows the waveforms of the motor current, the motor voltage and the motor speed during run-up at half-load and  $V_{ref} = 120$  volt for closed loop voltage stabilization using fuzzy logic control. It is observed that the response time is faster than when using the PI controller.

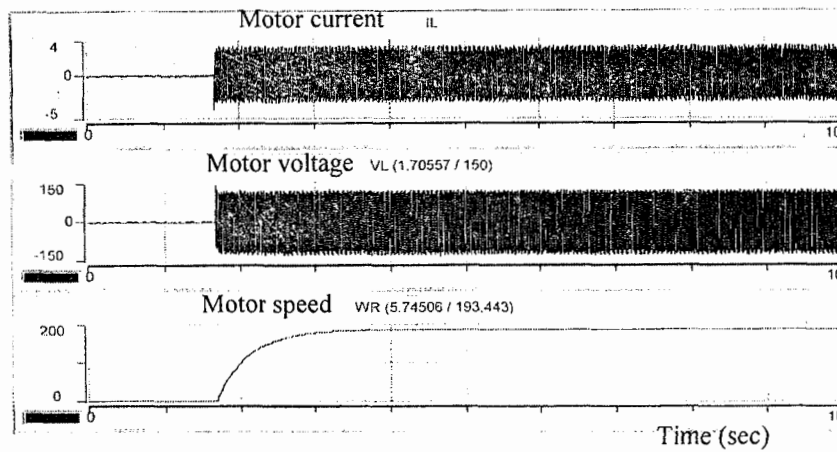


Fig. 14. Run-up behavior for half-load for closed loop voltage stabilization using fuzzy control

#### 5-3-4. Dynamic load change

Figures 15 and 16 show the motor voltage and speed response due to positive and negative change in load torque with  $V_{ref} = 120$  volt using fuzzy control. It is clear that the load voltage is constant and the time response is faster than when using the PI controller.

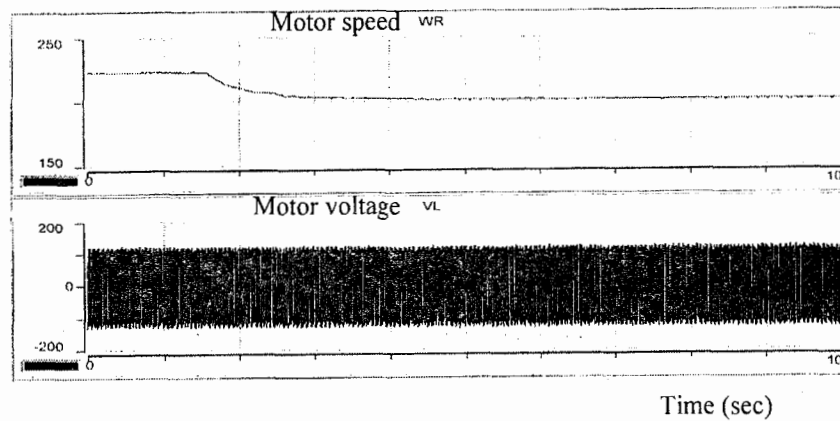


Fig. 15. Response due to a negative change in load torque using fuzzy control.

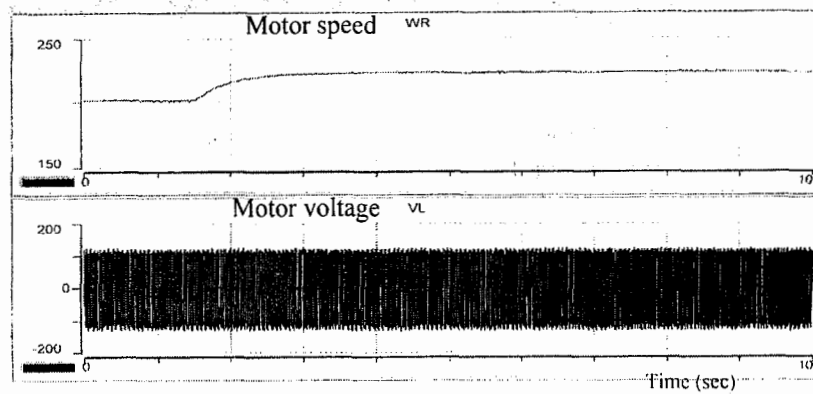


Fig. 16. Response due to a positive change in load torque using fuzzy control.

## 6. Harmonics calculation

Figures 17 and 18, show the variation of the simulation and experimental results of the total harmonic distortion factor in the load voltage and supply current with the control voltage. Figure 19 shows the simulation and experimental results for the variation of the common coupling bus-bar power factor versus the control voltage. It is observed that the total harmonic distortion for the load voltage and supply current are small and the power factor is near unity over the control range. \*

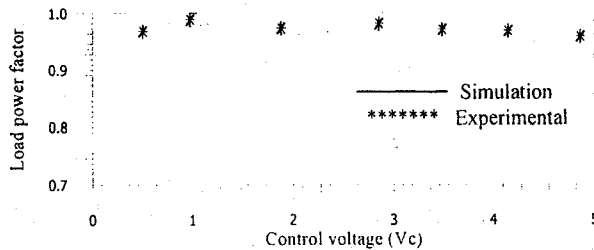


Fig. 17. Variation of the total harmonic distortion factor in the load voltage versus control voltage

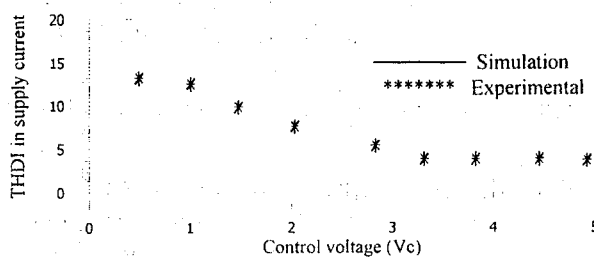


Fig. 18. Variation of the total harmonic distortion factor in supply current versus control voltage

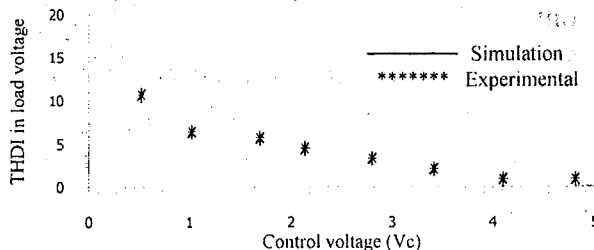


Fig. 19. Variation of the common bus bar power factor versus control voltage

## 7. CONCLUSIONS

A new simplified PWM control technique is proposed with switched reactor in parallel with a capacitor for static VAR compensation. The proposed technique is for load voltage stabilization, reactive power compensation and power factor improvement in the presence of feeder impedance. Suitable parameters of the

designed system are selected. The load terminal voltage, the load current and the supply current are shown to be close to the sinusoidal form.

The total harmonic distortion for load voltage and supply current are small. The power factor is improved and the results have shown that nearly unity power factor can be achieved. The experimental and simulation results indicate that the developed model has a high degree of accuracy in predicting both transient and steady-state performance.

The proposed system is fully controlled using the digital signal processor board. The proportional integral voltage controller parameters are given to stabilize the common coupling bus-bar voltage. Moreover, the experimental study using DSP clearly indicates the superior performance of fuzzy logic control for static and or dynamic load. This is because, it is inherently adaptive in nature. By good choice of control parameters, the fuzzy controller can give better results than the PI controller. Fuzzy control of the complete system gives good response in both motor run-up and during disturbances.

## REFERENCES

- [1] L. Moran, P. D. Ziogas, and G. Joos, "A Solid-State High-Performance Reactive-Power Compensator," *IEEE Transaction On Industry Application*, Vol. 29, NO.5, September /October 1993, pp. 969-978.
- [2] C. R. Vidyashankar, and A. K. Khargekar, "A Practical Fast Acting Control Scheme For Static VAR Compensator," *Electric Machines and Power Systems*, Vol. 1, 1986, pp 357-366
- [3] G. Joos, L. Moran, and P. D. Ziogas, "Performance Analysis of a PWM Inverter VAR Compensator," *Trans. Power Electronic*, Vol. 6, No. 8, July 1991, pp. 380-391.
- [4] S. S. Shokralla, "A new Simplified Approach For Load Voltage Stabilization Using Controlled Static VAR Compensation" *Alazher Second International Conference*, Cairo, Egypt, Dec. 21-24, 1991, pp. 976-987.
- [5] J. B. Ekanayake, N. Jenkins, and C. B. Cooper, "Experimental Investigation of an Advanced Static VAR Compensator," *IEEE Proc. Gener. Trans. Disturb.*, Vol.142, No.2, March 1995, pp. 202-210.
- [6] H. Jin, G. Goosand. Lopes, "An Efficient Switched-Reactor Based Static VAR Compensation," *IEEE Ind. Applicat.* Vol. 30, No.4, July/ Aug.1994, PP.998-1005.
- [7] A. A. Amin, "A Three-phase Foure-Wire Advanced Static VAR Compensator," *MEPCON'2000*, March28-30, cairo, Egypt, 2000, pp. 44-48.
- [8] A. M. Sharaf, M. Z. El-Sadek, F. N. Abd-Elbar, and A. M. Hemeida, "A Novel Error Driven Nonlinear Control Strategy For Transient Stability Enhancement Using Static VAR Compensators," *MEPCON'2000*, March 28-30, Cairo, Egypt, 2000, pp. 223-227.
- [9] M. El-Shebiny, and S.S.Shokralla, "Improvement of Induction Motor Performance Using Controlled Static VAR Compensator," *Eng. Research Bulletin*, Menuofya Unversity, Vol. 22, No.2, 1999, pp. 117-133.

- [10] E. E. El-Sabbe, E. E. El-Kholy, S. S. Shokran, and Nancy A. El-Heinawy, "A New Simplified Approach for Voltage Stabilization using Switched Reactr-Based Static VAR Compensator," MEPCON'2001, Dec. 29-31, Cairo, Egypt, 2000, pp. 691-696.
- [11] DSP - CI Teco Hardware, DSPACE Digital Signal Processing GmbH, Germany, 1993.

## NOMENCLATURE

C	: Compensator capacitor, $\mu\text{f}$
F	: Motor viscous friction coefficient, Nm/rad/sec.
$I_s, i_s$	: R.M.S. and instantaneous supply current, Amp.
$L_s$	: Supply inductance, H
$L_\theta, L_l$	: Controlled coil and load inductance's, H
$R_\theta, R_l$	: Controlled coil and load resistance's, ohm
$R_s$	: Supply resistance, ohm
$V_s, v_s$	: R.M.S. and instantaneous supply voltage, Volt
$V_m, v_m$	: R.M.S. and instantaneous load terminal voltage, Volt.
$Z_L$	: Load impedance, ohms
$\phi_l$	: Load phase- angle, degree
$\omega$	: Angular frequency
$L_a, L_f$	: The armature and field of the motor inductance's, H
$R_a, R_f$	: The armature and field of the motor resistance's, ohm
J	: The moment of inertia, $\text{Kg.m}^2$
$T_e, T_l$	: The electromagnetic and the load torque, N.M
$K_p$	: Proprtional gain
$K_i$	: Integral gain

## APPENDIX

1- The parameter values of the designed system at 50 Hz are as follows:

$$\begin{aligned} R_l &= 25 \text{ ohm} & L_l &= 0.159 \text{ H} \\ R_\theta &= 2.5 \text{ ohm} & L_\theta &= 0.199 \text{ H} \\ R_s &= 2.5 \text{ ohm} & L_s &= 0.027 \text{ H} \\ C &= 55 \mu\text{f} \end{aligned}$$

2- The test motor data and parameters:

1/3 HP, 220 v, 1.9 A, 6000 r.p.m,

Universal motor has the following measured parameters:

$$\begin{aligned} R_a + R_f &= 13.7 \text{ ohm}, & L_a + L_f &= 0.169 \text{ H}, \\ F &= 0.00012 \text{ NM/rad/sec}, \\ J &= 0.003 \text{ Kg.m}^2 \end{aligned}$$

## تطبيق معالج الإشارات الرقمية المعتمد على التحكم المنطقي المبهم فى تثبيت جهد الأطراف

د. / علوى عيسى الخولى و د. / عوض السيد عوض السبع  
أ.د. / شكرى سعد شكر الله و م. / نائسى عباس على الحفناوى

قسم الهندسة الكهربية كلية الهندسة جامعة المنوفية

### ملخص البحث:

يتضمن هذا البحث إقتراحا للنمذجة والتمثيل العددي وذلك لتثبيت جهد الحمل باستخدام التحكم فى الممانعة الموضوعية بالتوازي مع مكثف لتعويض القدرة الغير فعالة. ويتم التحكم باستخدام أسلوب تعديل عرض النبضة المنتظم وذلك للتحكم فى قيمة الممانعة وبالتالي قيمة التيار المار بها. وقد تم استخدام حمل إستاتيكي عبارة عن مقاومة وممانعة وحمل ديناميكي عبارة عن محرك عام وقد أخذت معاوقة المنبع والخط فى الإعتبار وتم إيجاد ثوابت النظام. ويمتاز هذا النظام المقترح بثبوت جهد الحمل وتحسين معامل القدرة الذى يقترب من الوحدة وأيضا إقتراب شكل موجه جهد الأطراف للحمل وتيار المنبع من الموجه الجيبية ويمتاز هذا النظام أيضا بتقليل التوافقيات لجهد الحمل مقارنة بالنظم السابقة وأيضا تم الحصول على أداء النظام لكل من حالة الاستقرار والحالة العابرة. وقد تم بناء هذا النظام معمليا لمقارنة النتائج النظرية بالعملية. وقد أثبتت وجود توافق كبير بينهما. وتعتبر الدراسة النظرية لهذا النظام أداة قوية للتنبؤ بسلوك مثل هذا النظام أو أى نظام آخر له ثوابت أخرى. كما تم بناء النظام المعملى باستخدام معالج الإشارات وتم الحصول على داله الانتقال لهذا النظام وذلك للحصول على ثوابت المحكم التكاملى التناسبى للجهد للحصول على تشغيل مستقر للنظام وأداء سريع عند تغير الحمل. ويشتمل البحث على استخدام التحكم المنطقي المبهم المبنى على أساس تثبيت جهد أطراف الحمل وذلك لحمل إستاتيكي أو حمل ديناميكي وتم إختيار ثوابت النظام الذى يمتاز بطبيعة التوانم الذاتى ليعطى نتائج أفضل للاستجابة بالمقارنة مع المحكم التكاملى التناسبى.